

A *Macaca mulatta* model of fulminant hepatic failure

Ping Zhou, Jie Xia, Gang Guo, Zi-Xing Huang, Qiang Lu, Li Li, Hong-Xia Li, Yu-Jun Shi, Hong Bu

Ping Zhou, Hong Bu, Department of Pathology, West China Hospital, Sichuan University, Chengdu 610041, Sichuan Province, China

Jie Xia, Gang Guo, Li Li, Yu-Jun Shi, Hong Bu, Key Laboratory of Transplant Engineering and Immunology, Ministry of Health, West China Hospital, Sichuan University, Chengdu 610041, Sichuan Province, China

Zi-Xing Huang, Department of Radiology, West China Hospital, Sichuan University, Chengdu 610041, Sichuan Province, China

Qiang Lu, Department of Ultrasound, West China Hospital, Sichuan University, Chengdu 610041, Sichuan Province, China

Hong-Xia Li, The National Chengdu Center for Safety Evaluation of Drugs, West China Hospital, Sichuan University, Chengdu 610041, Sichuan Province, China

Author contributions: Zhou P, Shi YJ and Bu H designed the project; Zhou P, Xia J, Guo G and Shi YJ performed the experiments; Zhou P and Shi YJ contributed to the discussion of the data and wrote the manuscript; Huang ZX contributed to the MRI examination; Lu Q contributed to the ultrasound examination; Li L contributed to the production and staining of section; Li HX provided the experimental animals and contributed to the biochemical examination.

Supported by National Basic Research Program of China, No. 2009CB522401; and grand from Natural Science Foundation of China, No. 30870983 and 30971118

Correspondence to: Yu-Jun Shi, MD, PhD, Key Laboratory of Transplant Engineering and Immunology, Ministry of Health, West China Hospital, Sichuan University, No. 1 Keyuan 4th Road, Chengdu 610041, Sichuan Province,

China. shiyujun@scu.edu.cn

Telephone: +86-28-85164030 Fax: +86-28-85164034

Received: May 19, 2011 Revised: June 23, 2011

Accepted: June 30, 2011

Published online: February 7, 2012

Abstract

AIM: To establish an appropriate primate model of fulminant hepatic failure (FHF).

METHODS: We have, for the first time, established a large animal model of FHF in *Macaca mulatta* by intra-

peritoneal infusion of amatoxin and endotoxin. Clinical features, biochemical indexes, histopathology and iconography were examined to dynamically investigate the progress and outcome of the animal model.

RESULTS: Our results showed that the enzymes and serum bilirubin were markedly increased and the enzyme-bilirubin segregation emerged 36 h after toxin administration. Coagulation activity was significantly decreased. Gradually deteriorated parenchymal abnormality was detected by magnetic resonance imaging (MRI) and ultrasonography at 48 h. The liver biopsy showed marked hepatocyte steatosis and massive parenchymal necrosis at 36 h and 49 h, respectively. The autopsy showed typical yellow atrophy of the liver. Hepatic encephalopathy of the models was also confirmed by hepatic coma, MRI and pathological changes of cerebral edema. The lethal effects of the extrahepatic organ dysfunction were ruled out by their biochemical indices, imaging and histopathology.

CONCLUSION: We have established an appropriate large primate model of FHF, which is closely similar to clinic cases, and can be used for investigation of the mechanism of FHF and for evaluation of potential medical therapies.

© 2012 Baishideng. All rights reserved.

Key words: Fulminant hepatic failure; *Macaca mulatta*; Biochemistry; Imaging; Pathology

Peer reviewer: Dr. Yasuji Arase, Department of Gastroenterology, Toranomon Hospital, 2-2-2 Toranomon Minato-ku, Tokyo 105-8470, Japan

Zhou P, Xia J, Guo G, Huang ZX, Lu Q, Li L, Li HX, Shi YJ, Bu H. A *Macaca mulatta* model of fulminant hepatic failure. *World J Gastroenterol* 2012; 18(5): 435-444 Available from: URL: <http://www.wjgnet.com/1007-9327/full/v18/i5/435.htm> DOI: <http://dx.doi.org/10.3748/wjg.v18.i5.435>

INTRODUCTION

Fulminant hepatic failure (FHF) is an uncommon and challenging clinical disease characterized by sudden and severe hepatic injury and dysfunction, with many different symptoms and complications, and high mortality. The term was first used in 1970 to describe a potentially reversible disorder that was the result of severe liver injury in the absence of pre-existing liver disease, with an onset of encephalopathy within 8 wk of symptom appearance^[1]. The incidence and etiology of FHF vary according to different geographic regions^[1,2], and viral hepatitis and drug or toxin ingestion are the most common causes. As the pathophysiological changes are complicated and still need to be investigated, a clinically relevant large-animal model would be an indispensable tool. Orthotopic liver transplantation has been proved to be an effective treatment^[3-6], but the shortage of donor organs has restricted its wide application^[7-9]. The development of new therapies, including hepatocyte transplantation, stem cell transplantation, tissue engineered liver and bioartificial liver support systems, is still under investigation^[3-6]. Before these treatments can be used clinically, their effects should be determined in large animal models. For a satisfactory animal model of FHF, seven criteria were suggested by Terblanche *et al*^[10] and Fourneau *et al*^[11]: (1) reversibility; (2) reproducibility; (3) death from liver failure; (4) presence of a therapeutic window; (5) a large animal model; (6) minimal hazard to personnel; and (7) a conscious animal model. Previous reports have described different animal models of FHF induced by various methods^[7,12,13], but all the established models did not entirely satisfy all these criteria. Moreover, selection of a species with similar metabolic and physiological properties to humans is of importance. In this article, we describe, for the first time, the establishment of a *Macaca mulatta* model of FHF and the dynamic biochemical, pathological and imaging changes are also described.

MATERIALS AND METHODS

Chemicals

Lipopolysaccharide (LPS) from *Escherichia coli* was purchased from Sigma-Aldrich, Inc., St. Louis, MO. α -amanitin was from Alexis Biochemicals Co., Lausen, Switzerland. Gd-BOPTA (multihance) and SonoVue, contrast media for magnetic resonance imaging (MRI) and ultrasonography, respectively, were from Bracco Sine Pharmaceutical Co., Shanghai, China.

Animals

Two healthy female *Macaca mulattas*, 3 and 4 years old and with body weights of 5.5 kg and 4.6 kg, respectively, were purchased from the Safe and Secure Experimental Animal Breeding Base in Chengdu, China. They were housed in a large animal care facility with a constant temperature of 20 °C \pm 1 °C and a 6 am to 6 pm light cycle. Two weeks were allowed for the animals to acclimatize to

the animal facility before the study. They were fed with standard dry monkey food, washed apples and water *ad libitum*. Animal procedures and care were conducted in accordance with the institutional guidelines and in compliance with national and international laws and policies.

Study design

After premedication with ketamine (15 mg/kg im), skin preparation was performed on the posterior legs for blood collection from the saphenous vein and on the abdomen for intraperitoneal infusion and hepatic needle biopsy. LPS (1 μ g/kg) and α -amanitin (0.1 mg/kg) were mixed in 50 mL physiological saline and slowly infused into the peritoneal cavity. Before their administration, blood biochemical parameters of the liver, kidney, heart and pancreas were measured, and total body MRI and ultrasonography were performed to acquire the physiological data as baseline values (expressed as "0" in the figures). After administration, blood biochemical parameters were measured every 12 h. An imaging examination was performed every 24 h.

Core needle biopsy of the liver guided by ultrasonography scan was performed 12 h after administration and repeated every 24 h. Part of the needle biopsy specimens was subjected to frozen section and oil red O staining.

The state of consciousness and behavior of the animals was observed and the hepatic encephalopathy was defined according to the West-Haven criteria in humans^[14].

The two *Macaca mulattas* underwent necropsies after death, which included a full macroscopy and a histological evaluation of the liver, kidneys, lungs, heart, brain, spleen, pancreas and lymph nodes. Tissues were fixed in 10% neutral buffered formalin, sectioned at 5 μ m and stained with hematoxylin and eosin (H and E).

RESULTS

Clinical features and animal survival

The animals showed a gradual increase in listlessness and loss of appetite after toxin administration. Anorexia and vomiting occurred 24 h after administration, followed by grasping disability, mental indifference, drowsiness and coma. Hepatic coma appeared at 42 h and 56 h, and death occurred at 49 h and 70 h, respectively.

Biochemical results

We measured the liver enzymes, bilirubin and coagulation indices to determine the extent of liver injury. The data below were the average values from the two *Macaca mulatta* models when both were alive, or from one monkey when one died. After administration, the values of alanine aminotransferase and aspartate aminotransferase began to increase significantly and reached a peak at 36 h with over 300-fold and 200-fold increases from the baseline, respectively (Figure 1A), then the values sharply decreased. The total bilirubin, direct bilirubin and indirect bilirubin all increased gradually, and the final measured values exceeded a 30-fold rise from the corresponding

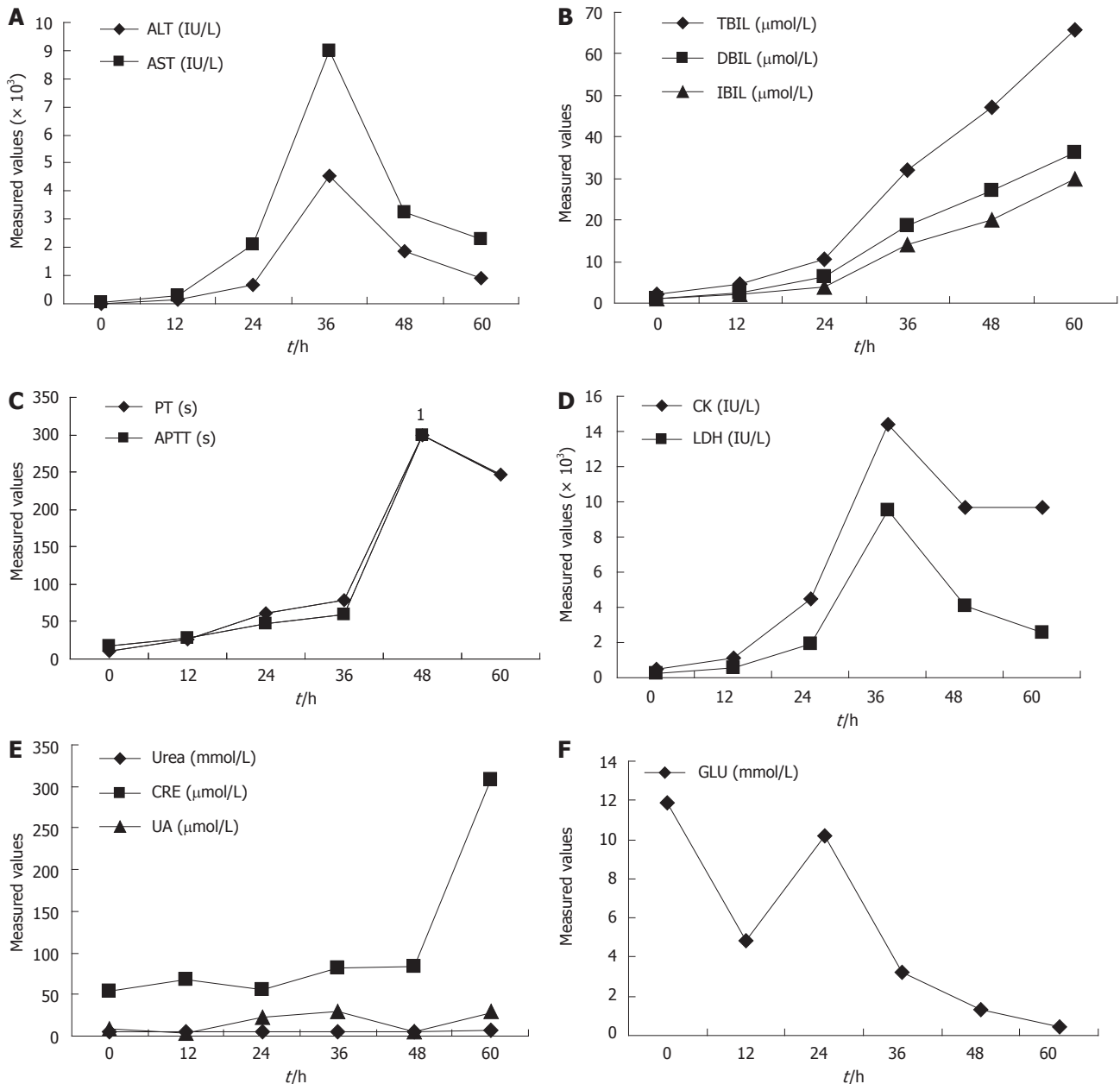


Figure 1 Blood biochemical parameters of the *Macaca mulatta* model of fulminant hepatic failure. The abscissa and ordinate represent measured time and value, respectively. ALT: Alanine aminotransferase; AST: Aspartate aminotransferase; TBIL: Total bilirubin; DBIL: Direct bilirubin; IBIL: Indirect bilirubin; PT: Prothrombin time; APTT: Activated partial thromboplastin time; CK: Creatine kinase; LDH: Lactate dehydrogenase; CRE: Creatinine; UA: Uric acid; GLU: Glucose; FHF: Fulminant hepatic failure. *Represents values > 300 s, which exceeded the range of the equipment, so we did not obtain an exact measurement.

baseline values (Figure 1B). The consistent increase in bilirubin and the notable decrease in enzymes after 36 h suggest the emergence of enzyme-bilirubin segregation. The prothrombin time (PT) and activated partial thromboplastin time (APTT) were also prolonged after administration. At 48 h, both the levels exceeded 300 s so that we could not measure the exact number using the machine. Even the last two measured levels of PT and APTT showed little diminution, and at 250 s were still 14- to 22-fold of the baseline (Figure 1C). The ratios of prothrombin activity were 1.18% and 5.53%.

To determine whether the toxins damaged other organs, the biochemical parameters of the heart, kidneys

and pancreas were measured. Creatine kinase (CK) and lactate dehydrogenase (LDH), markers of myocardial injury, also displayed peaks at 36 h with values 27-fold and 38-fold that of baseline, respectively (Figure 1D). Of the three kidney-associated parameters, i.e., urea, creatinine (CRE) and uric acid, only the level of CRE obviously increased after 48 h (Figure 1E). The blood glucose concentration decreased (Figure 1F), and the serum amylase of the pancreas did not show any significant changes.

Imaging

MRI and ultrasonography were performed every 24 h, and the final scans were performed when the animal

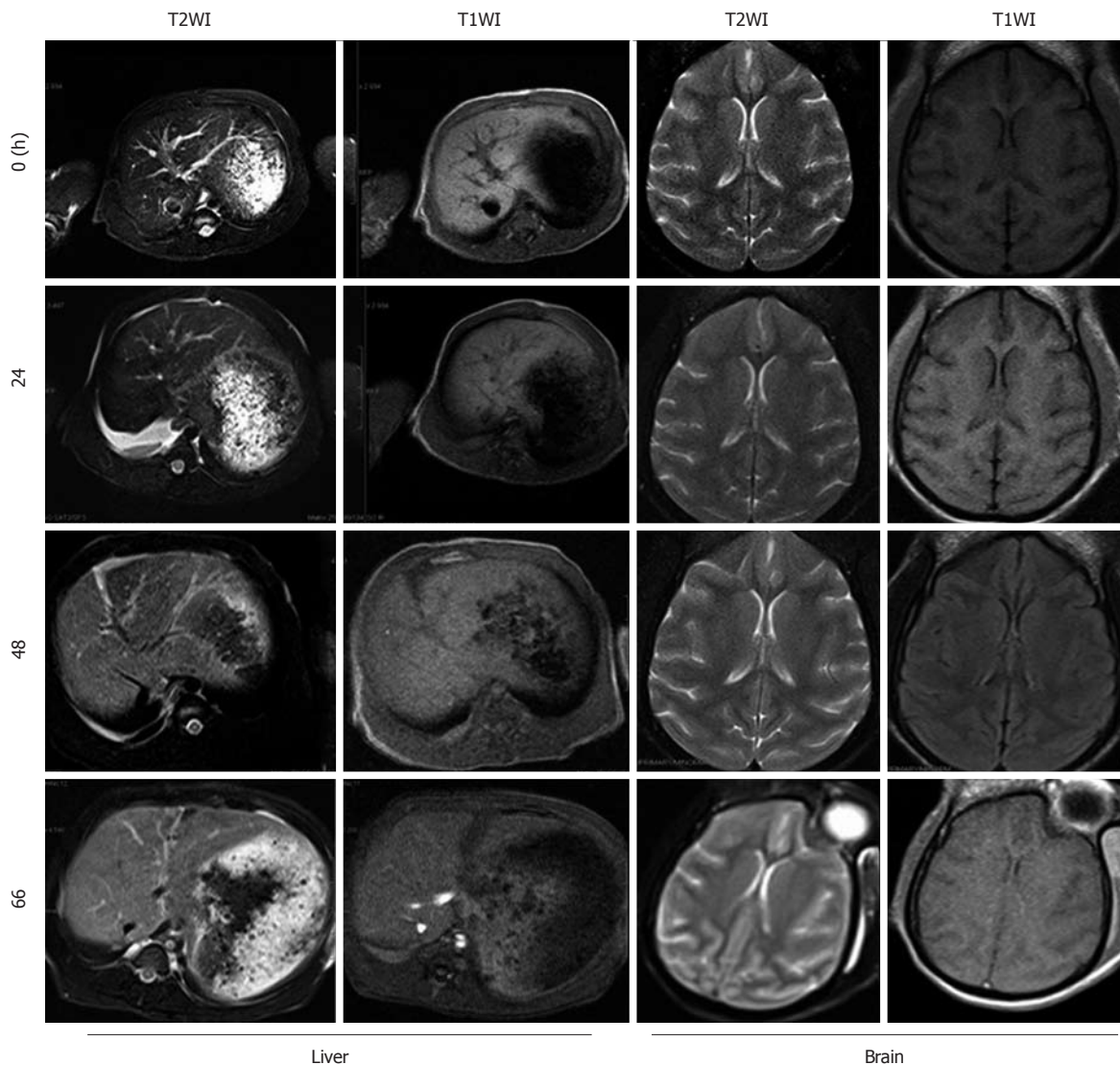


Figure 2 Magnetic resonance imaging of the liver and brain of *Macaca mulatta* model at different times. T2WI: T2-weighted imaging; T1WI: T1-weighted imaging.

died. At 24 h, MRI showed slight signals emerging in the left lobe of the liver, and Gd-enhanced T1-weighted imaging demonstrated homogeneous intensity. The signal began to increase heterogeneously in the parenchyma at 48 h, and became more heterogeneous and diffuse at 66 h, and the intensity decreased on a widespread basis in the hepatobiliary period (Figure 2). In ultrasonography, the echo of the liver parenchyma was slightly enhanced at 48 h, especially in the left lobe, and the contrast sonogram with SonoVue showed low perfusion. The hepatic artery resistance index increased. At 60 h, the echo was still enhanced slightly, but the portal vein velocity decreased and the hepatic artery resistance index increased further (Figure 3). Before 48 h, no predominant changes were found in brain MRI, but at 66 h, abnormal rhythmic signals emerged in the frontal lobe and both temporal lobes, which demonstrated hyperacute ischemia (Figure 2). We also scanned the thoracic and abdominal organs and no marked abnormality was found (data not shown).

Pathological changes

Core needle biopsies were performed at 12 h and 36 h af-

ter administration and the animals underwent necropsies after death. The main organs were evaluated, including the liver, kidneys, lungs, heart, brain, spleen, pancreas and lymph nodes, for macroscopic and histological changes.

H and E and oil red O staining showed that the liver developed severe steatosis at 36 h after toxin infusion, and in the necropsy liver, extensive parenchymal necrosis was found. The hepatic cord was dissociated, with disordered hepatocytes, and the hepatic sinusoid was extended with hyperemia. Vacuoles appeared in the cytoplasm, and patchy necrosis was found in the portal areas. In the non-necrotic areas, most hepatocytes were stained reddish-orange by oil red O. In the necropsy section, massive necrosis caused loss of almost all of the hepatocytes, and only the reticular structure remained, which is similar to the case in humans suffering from acute severe viral hepatitis (Figure 4).

With the naked eye, the livers appeared softer and smaller, with sharper and thinner edges, than the normal liver. The surface color was red and yellow, and it was a uniform yellow at the cut surface (Figure 4). Vascular dilatation and hyperemia were found on the surface of

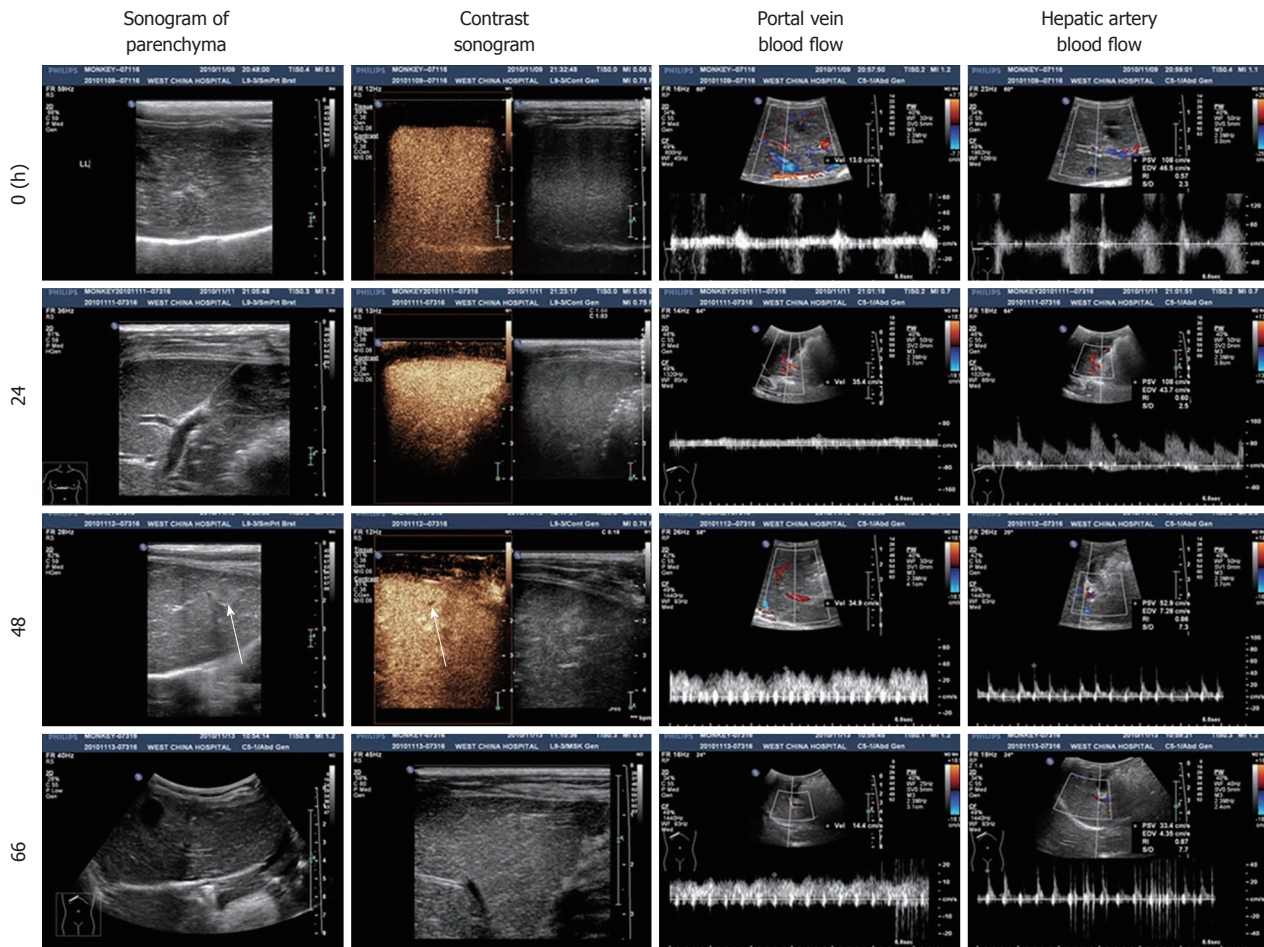


Figure 3 Liver sonogram of the *Macaca mulatta* model at different times. Arrows show a slightly enhanced echo and lower perfusion of SonoVue at 48 h.

the brain and cerebral edema was proved by widened gyri and shallowed sulci (Figure 5). Under microscopy, the superficial layer of the brain was loose, edematous and weakly stained (Figure 6).

Both kidneys showed hyperemia. The heart, spleen and pancreas did not display obvious gross changes (Figure 5). No peritoneal hyperemia, adhesions or edema in the peritoneal cavity was found. The lymph nodes located in the mesentery were enlarged and darkened. Under microscopy, they showed diffuse bleeding and lymphocytes were extensively reduced with much histiocyte proliferation. Arterioles in the lymphoid follicles were found to have hyaline degeneration. Both kidneys were also injured and demonstrated ectasia and hyperemia of the capillaries in the renal glomerulus and the stroma of the kidney tubules, and there was cellular swelling in the tubule epithelial cells. Only a wave-like change of the myocardium was found in the heart (Figure 6).

DISCUSSION

In this study, we have established, for the first time, a *Macaca mulatta* model of FHF, which satisfies all of the criteria for a large animal model of FHF proposed by Terblanche *et al*^[10] and Fourneau *et al*^[11], especially a con-

scious animal model for observation of the development of hepatic encephalopathy. All the clinical features and biochemical parameters, including liver enzymes, bilirubin as well as coagulation activity, confirmed that this model matched all the diagnostic criteria of human FHF. In addition, we dynamically examined and recorded the pathological and imaging changes in the liver and extrahepatic organs during disease progression.

Animal models of FHF are urgently needed to fully investigate the pathogenesis, progression, diagnosis and treatment of this serious disease clinically. Novel therapeutic strategies including hepatocyte transplantation, stem cell transplantation, tissue engineered liver and bioartificial liver support systems are under investigation. However, all the therapies need to be tested in an animal model before clinic use. Over the past 30 years, various animal models of FHF have been created with different methods^[7,12,13], including models using rodents^[15-18], dogs^[19-23] and pigs^[24,25]. However, differences in the metabolic and physiological properties in these distantly relative species restricted the application of the results to humans. As the closest relative to the human, the primate possesses much more similar metabolic and physiological properties, and a primate with FHF is considered to be the best large animal model for use in basic and pre-clin-

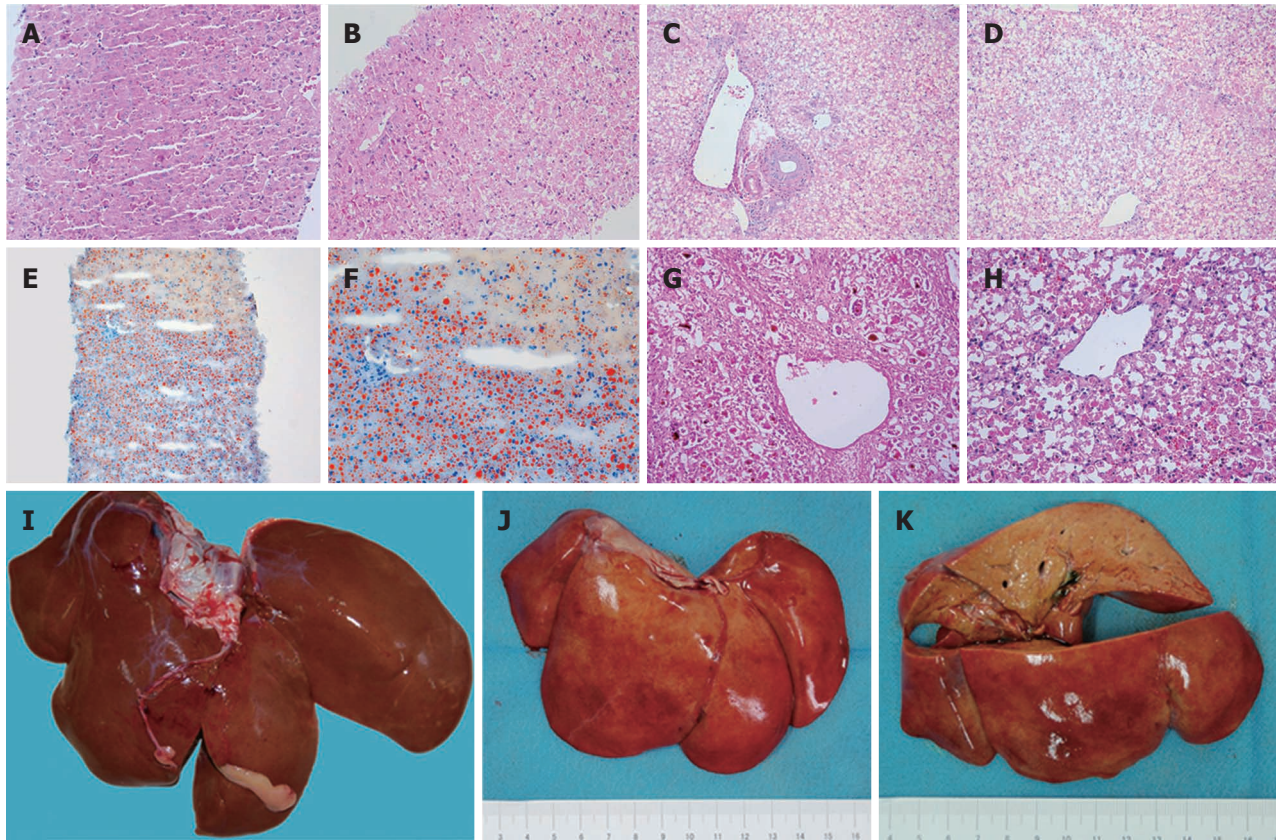


Figure 4 Histopathological changes of the liver. A: Tissue from needle biopsy at 12 h. Changes in organizational structure and cell morphology were not obvious [hematoxylin and eosin (H and E) stain, $\times 200$]; B: Tissue from needle biopsy at 36 h. Vacuoles appeared in the hepatocellular cytoplasm (H and E stain, $\times 200$); C, D: Tissue from necropsy after death at 70 h. Hepatocellular necrosis was distributed in the portal area (C) and central area (D) (H and E stain, $\times 200$). Massive necrosis caused almost all of the hepatocytes to be lost, and only the support structure remained; E: Frozen tissue from needle biopsy at 36 h. The extensive reddish-orange color suggested serious fatty degeneration (oil red O stain, $\times 100$); F: Frozen tissue from needle biopsy at 36 h. In the borderline between necrosis and steatosis, the reddish-orange color was obvious (oil red O stain, $\times 200$); G, H: Comparison of pathological changes of fulminant hepatic failure in humans induced by viral hepatitis (G) and a *Macaca mulatta* model induced by α -amanitin and lipopolysaccharide (H) (H and E stain, $\times 200$); I: Normal liver of *Macaca mulatta* for comparison; J: The surface view of the experimental liver on necropsy appeared red and yellow; K: The cut surface view of the experimental liver was uniformly yellow.

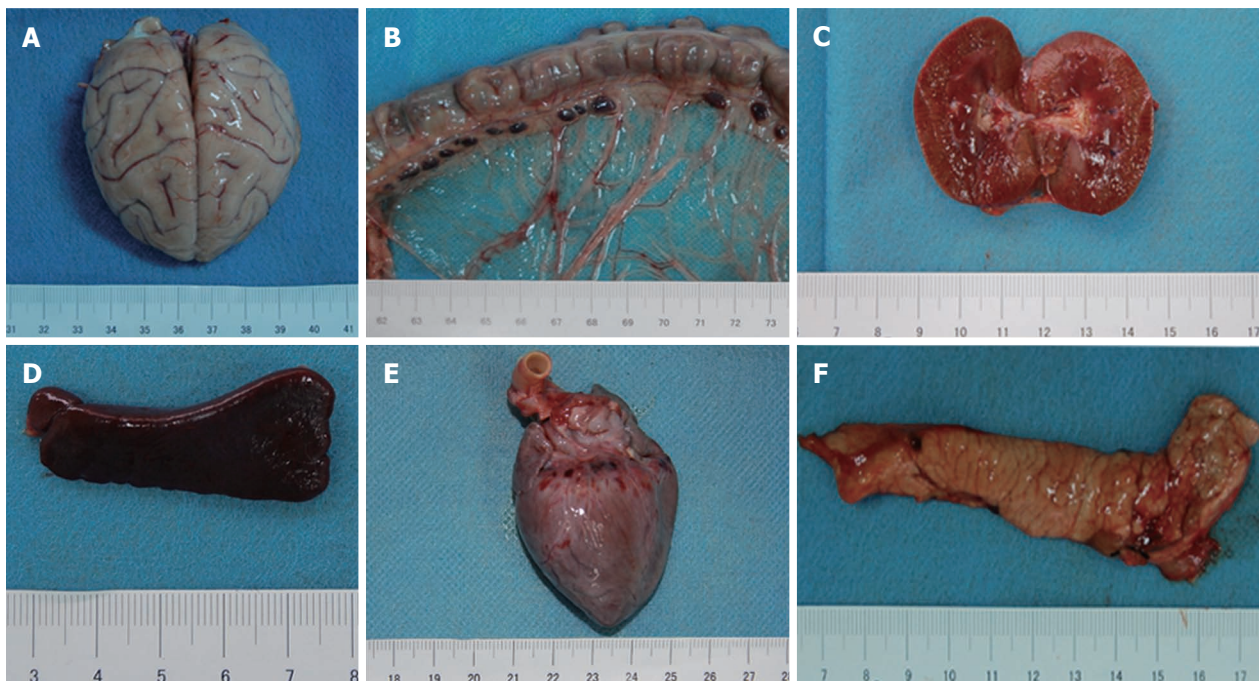


Figure 5 Other main organs on necropsy. A: The brain with cerebral edema; B: Mesenteric lymph nodes enlarged and beaded; Hyperemia of the kidney (C), spleen (D), heart (E), and pancreas (F) without obvious gross lesions.

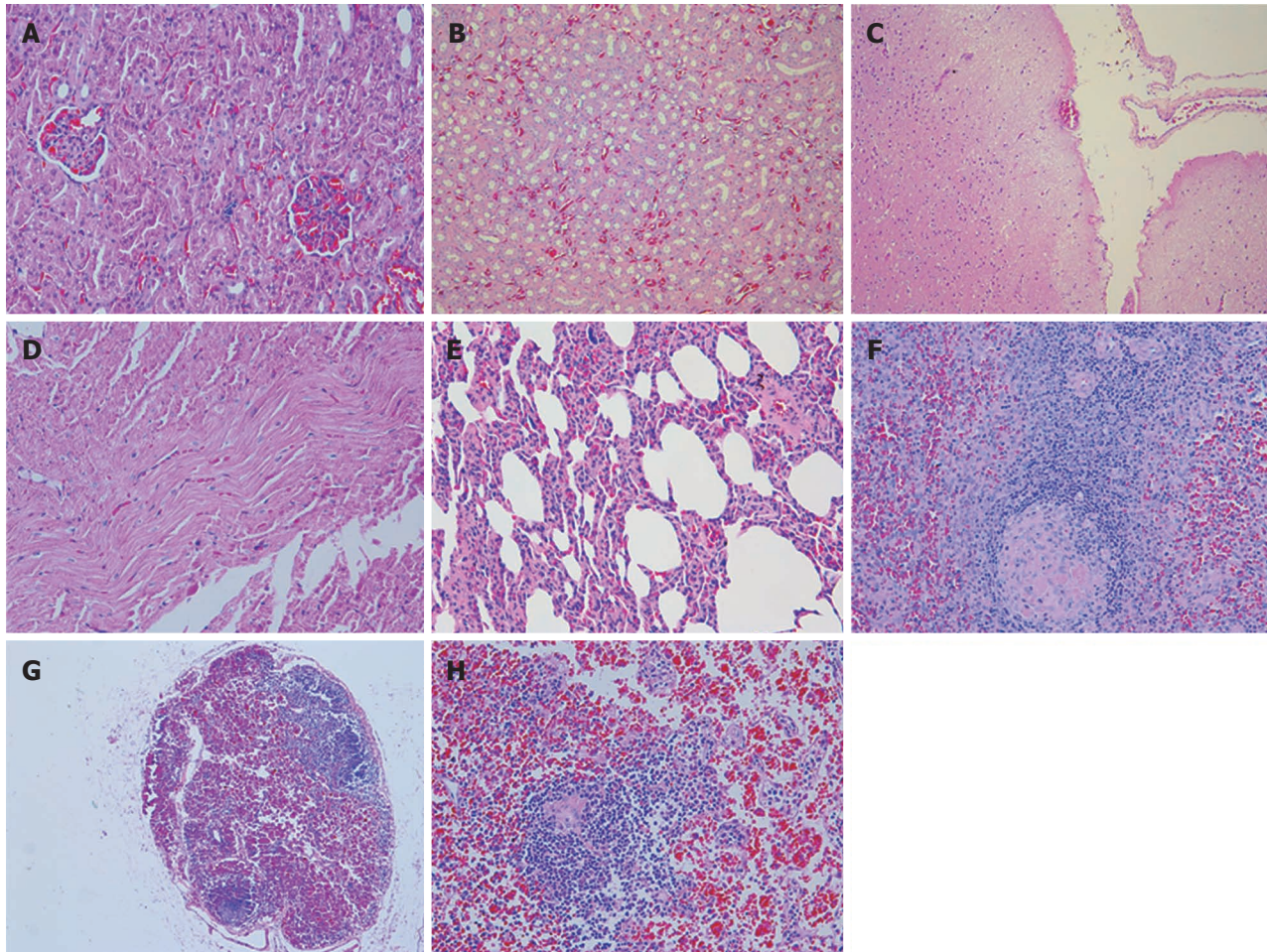


Figure 6 Histopathological changes of other organs. A: Ectasia and hyperemia of capillaries in the renal glomerulus [hematoxylin and eosin (H and E) stain, $\times 200$]; B: Widespread hyperemia of capillaries in the renal stroma and cellular swelling in the tubular epithelial cells (H and E stain, $\times 100$); C: Weak staining in the superficial layer of the brain suggest cerebral edema (H and E stain, $\times 100$); D: Wave-like changes in the myocardium (H and E stain, $\times 200$); E: Hyperemia of capillaries in the stroma and hyaline changes in the arterioles of the lung (H and E stain, $\times 200$); F: Hyaline changes in the central artery of the spleen (H and E stain, $\times 200$); G: Widespread reduction in lymphocytes and hemorrhage in the mesenteric lymph nodes (H and E stain, $\times 50$); H: Hemorrhage and histiocyte proliferation in the mesenteric lymph nodes. Hyaline change appeared in the vessel wall of lymphoid follicles (H and E stain, $\times 200$).

ical research. To the best of our knowledge, our *Macaca mulatta* model of FHF is the first large primate model in this field.

Methods used to induce the FHF models included surgical intervention and hepatotoxin administration. Total or partial hepatectomy and hepatic ischemic injury were widely used, but these relied on extensive surgical expertise and were influenced by individual variations in the animals. Hepatotoxins, which induce massive hepatic necrosis, are widely used in the establishment of a FHF model. Acetaminophen and galactosamine were the two most widely used hepatotoxins^[17,19,22,26-31], and in some studies, carbon tetrachloride^[32], thioacetamide^[33,34], azoxymethane^[35,36], concanavalin A^[37] and amanita phalloides^[38,39] were also employed. However, a lack of standardization, especially a lack of reproducibility, is the major disadvantage of models induced by acetaminophen^[7,10]. The high costs restrict the application of galactosamine in large-scale models^[40]. Amatoxin, a polypeptide extracted from a hypertoxic mushroom, has been used as a hepatotoxin in pigs with an endotoxin (LPS), and this

model was reported to satisfy the criteria of near-universal mortality from highly reproducible hepatic failure, of mortality occurring in a defined time range, of damage specific to the liver, and of potential for recovery of the damaged liver^[38,39]. In our preliminary experiment, LPS (2.25 $\mu\text{g}/\text{kg}$) and α -amanitin (0.225 mg/kg) were injected in a *Macaca mulatta* through a branch of the mesenteric vein by laparotomy at the dose converted from that used in pigs, which received LPS and α -amanitin at a dose of 1 $\mu\text{g}/\text{kg}$ and 0.1 mg/kg , respectively^[38,39]. However, the animal died within 8 h. We supposed that the direct and undiluted toxic effects to the liver might be the main cause of death and the surgery might promote the death of the *Macaca mulatta*. Thus, we reduced the dose of the two hepatotoxins to the level used in pigs, which was nearly half of our preliminary dose. We then improved the administration pathway by slow intraperitoneal infusion of the toxins diluted in 50 mL physiological saline instead of direct portal injection. Our results showed that the animals survived for at least 49 h and all the features of FHF were clearly presented. Most importantly, the

prolonged disease course ensures a wide therapeutic window. It is possible that intraperitoneal infusion of toxins could lead to severe peritonitis. Fortunately, we did not find any symptoms and signs of peritonitis, either in imaging examination or in necropsy.

Induced by α -amanitin and LPS, the hepatocytes presented severe steatosis first and massive necrosis at the end stage of FHF, which is similar to the case in humans suffering from acute severe viral hepatitis. Serum parameters, including hepatic enzymes, bilirubin, and coagulation activities, as well as serum ammonia, are often considered as the markers representing the level of damage of hepatocytes, since a biopsy is seldom carried out because of the restriction of invasive operation and bleeding. In fact, the hepatic injury during the course of FHF still needs direct confirmation. Our model offers an appropriate model to obtain real-time pathological changes in the hepatocytes, which makes it valuable for study of clinical features based on the pathological changes.

We also monitored the continuous alteration of the liver by imaging, and this is the first report on dynamic MRI of the liver during the course of FHF, either in patients or in an animal model. Combining the biopsy and the MRI, it is feasible to establish the diagnostic criteria of the damage level based on the MRI values, thus offering a non-invasive strategy to reveal the level of hepatic injury.

Hepatic encephalopathy is one of the most important clinical features and causes of death of FHF. Being consanguineous with humans, the *Macaca mulatta* presents similar behavior and consciousness to humans suffering from FHF. In addition, the brain volume and the similar gyrus outline make it suitable for MRI examination of the cerebral edema, ischemia or infarction. In our model, the progressing symptoms of listlessness, anorexia, grasping disability, mental indifference, drowsiness and coma are fully developed and thoroughly recorded. The behavior and conscious alterations, combined with the MRI and pathological changes, make it a valuable model for further investigation of the pathogenesis and pathophysiology of hepatic encephalopathy, which could not be reproduced in humans or in any other animals. As a noninvasive means of detection, MRI may be an appropriate strategy to monitor the progression of the hepatic encephalopathy. The first objective assessment of MR brain changes specific to hepatic encephalopathy was made in the early 1990s. It was noted that in patients with cirrhosis, the basal ganglia appeared hyperintense on T1-weighted MRI^[41]. However, continuous data are still absent to reveal the correlation between the degree of encephalopathy and the MRI parameters during the course of FHF. With our model, it is feasible to obtain the dynamic imaging alterations during the whole course of hepatic encephalopathy.

It is necessary to rule out that animal death was induced by extrahepatic organ failure. In our experiment, the main extrahepatic organs were also evaluated. The in-

creasing of CRE happened late, suggesting that the damage to the kidneys was a result of hepatorenal syndrome rather than direct toxin damage. The values of CK and LDH increased immediately after toxin administration, but no marked abnormality was found by echocardiogram and no myocardial necrosis was observed in histopathological examination. The cause of the increased CK and LDH still needs clarification. The lesion of the mesenteric lymph nodes might be associated with the toxins, which needs further study. We did not find any pathological evidences indicating cell injury of the lung and pancreas. Above all, we can conclude that the toxicity of intraperitoneal infusion of amatoxin and endotoxin is liver-specific and animal death is directly correlated with FHF and not extrahepatic organ failure.

We describe, for the first time, a *Macaca mulatta* model of fulminant hepatic failure, which satisfies all of the criteria for a large animal model of FHF^[10,11]. With similar metabolic and physiological properties to humans, our primate animal model of FHF offers a valuable model to be used for investigation of the pathophysiology of FHF and for evaluation of potential medical therapies. Compared with other animals, primate models are more expensive, and the ethics of using such animals should be taken into consideration.

COMMENTS

Background

Fulminant hepatic failure (FHF) is an uncommon and challenging clinical disease characterized by sudden and severe hepatic injury and dysfunction, and it results in many different symptoms and complications with a high mortality. Previous reports have described different animal models of FHF induced by various methods, but all the established models did not entirely satisfy all the criteria.

Research frontiers

Animal models of FHF are urgently needed to fully investigate the pathogenesis, progression, diagnosis and treatment of this serious disease in the clinic. Recently, more studies have focused on large animal models and therapy for FHF. Novel therapeutic strategies including hepatocyte transplantation, stem cell transplantation, tissue engineered liver and BAL support systems are under investigation. Also, various animal models of FHF have been created with different methods, including models using rodents, dogs and pigs. However, differences in metabolic and physiological properties in these distantly relative species restricted the application of the results to humans. No primate animal model with FHF has been created before.

Innovations and breakthroughs

In this article, the authors describe, for the first time, a *Macaca mulatta* model of FHF, which satisfies all of the criteria for the large animal model of FHF. It is important that with the model, it is feasible to obtain dynamic imaging and pathologic alterations, and this is the first report about dynamic MRI of the liver during the course of FHF, either in patients or in animal models. Though lipopolysaccharide and α -amanitin were reported to induce a pig model of FHF, the main extrahepatic organs were not evaluated. In this article, the authors improved the administration pathway and evaluated the main extrahepatic organs.

Applications

The primate animal model of FHF offers a valuable model to be used for investigation of the mechanism of FHF and for evaluation of potential medical therapies.

Terminology

Macaca Mulatta: A species of the genus *MACACA* inhabiting India, China, and other parts of Asia. The species is used extensively in biomedical research and adapts very well to living with humans.

Peer review

The authors show an appropriate large primate model of fulminant hepatic failure. They described the rigid data of hepatic failure by biochemical results, imaging, and pathological changes. The primate animal model of fulminant hepatic failure has clinical benefit because of similar metabolic and physiological properties to human. This paper is an interesting and instructive manuscript. It is well written.

REFERENCES

- Bernal W**, Auzinger G, Dhawan A, Wendon J. Acute liver failure. *Lancet* 2010; **376**: 190-201
- Fontana RJ**. Acute liver failure including acetaminophen overdose. *Med Clin North Am* 2008; **92**: 761-794
- Adam R**, Cailliez V, Majno P, Karam V, McMaster P, Caine RY, O'Grady J, Pichlmayr R, Neuhaus P, Otte JB, Hoeckerstedt K, Bismuth H. Normalised intrinsic mortality risk in liver transplantation: European Liver Transplant Registry study. *Lancet* 2000; **356**: 621-627
- Lidofsky SD**, Bass NM, Prager MC, Washington DE, Read AE, Wright TL, Ascher NL, Roberts JP, Scharschmidt BF, Lake JR. Intracranial pressure monitoring and liver transplantation for fulminant hepatic failure. *Hepatology* 1992; **16**: 1-7
- de Rave S**, Tilanus HW, van der Linden J, de Man RA, van der Berg B, Hop WC, Ijzermans JN, Zondervan PE, Metseelaar HJ. The importance of orthotopic liver transplantation in acute hepatic failure. *Transpl Int* 2002; **15**: 29-33
- Wall WJ**, Adams PC. Liver transplantation for fulminant hepatic failure: North American experience. *Liver Transpl Surg* 1995; **1**: 178-182
- Newsome PN**, Plevris JN, Nelson LJ, Hayes PC. Animal models of fulminant hepatic failure: a critical evaluation. *Liver Transpl* 2000; **6**: 21-31
- Nussler A**, Konig S, Ott M, Sokal E, Christ B, Thasler W, Brulport M, Gabelein G, Schormann W, Schulze M, Ellis E, Kraemer M, Nocken F, Fleig W, Manns M, Strom SC, Hengstler JG. Present status and perspectives of cell-based therapies for liver diseases. *J Hepatol* 2006; **45**: 144-159
- Stravitz RT**. Critical management decisions in patients with acute liver failure. *Chest* 2008; **134**: 1092-1102
- Terblanche J**, Hickman R. Animal models of fulminant hepatic failure. *Dig Dis Sci* 1991; **36**: 770-774
- Fourneau I**. A model to test the efficiency of a bioartificial liver. In: A potential reversible model of acute liver failure in the pig. Belgium: Leuven University Press, 2001; 41-56
- van de Kerkhove MP**, Hoekstra R, van Gulik TM, Chamuleau RA. Large animal models of fulminant hepatic failure in artificial and bioartificial liver support research. *Biomaterials* 2004; **25**: 1613-1625
- Tuñón MJ**, Alvarez M, Culebras JM, González-Gallego J. An overview of animal models for investigating the pathogenesis and therapeutic strategies in acute hepatic failure. *World J Gastroenterol* 2009; **15**: 3086-3098
- Ferenci P**, Lockwood A, Mullen K, Tarter R, Weissenborn K, Blei AT. Hepatic encephalopathy—definition, nomenclature, diagnosis, and quantification: final report of the working party at the 11th World Congresses of Gastroenterology, Vienna, 1998. *Hepatology* 2002; **35**: 716-721
- Walker RM**, Racz WJ, McElligott TF. Acetaminophen-induced hepatotoxicity in mice. *Lab Invest* 1980; **42**: 181-189
- Olafsson S**, Gottstein J, Blei AT. Brain edema and intracranial hypertension in rats after total hepatectomy. *Gastroenterology* 1995; **108**: 1097-1103
- Blitzer BL**, Waggoner JG, Jones EA, Gralnick HR, Towne D, Butler J, Weise V, Kopin IJ, Walters I, Teychenne PF, Goodman DG, Berk PD. A model of fulminant hepatic failure in the rabbit. *Gastroenterology* 1978; **74**: 664-671
- Horowitz ME**, Schafer DF, Molnar P, Jones EA, Blasberg RG, Patlak CS, Waggoner J, Fenstermacher JD. Increased blood-brain transfer in a rabbit model of acute liver failure. *Gastroenterology* 1983; **84**: 1003-1011
- Francavilla A**, Makowka L, Polimeno L, Barone M, Demetris J, Prelich J, Van Thiel DH, Starzl TE. A dog model for acetaminophen-induced fulminant hepatic failure. *Gastroenterology* 1989; **96**: 470-478
- Kelly JH**, Koussayer T, He DE, Chong MG, Shang TA, Whisennand HH, Sussman NL. An improved model of acetaminophen-induced fulminant hepatic failure in dogs. *Hepatology* 1992; **15**: 329-335
- Rozga J**, Williams F, Ro MS, Neuzil DF, Giorgio TD, Backfisch G, Moscioni AD, Hakim R, Demetriou AA. Development of a bioartificial liver: properties and function of a hollow-fiber module inoculated with liver cells. *Hepatology* 1993; **17**: 258-265
- Sielaff TD**, Hu MY, Rollins MD, Bloomer JR, Amiot B, Hu WS, Cerra FB. An anesthetized model of lethal canine galactosamine fulminant hepatic failure. *Hepatology* 1995; **21**: 796-804
- Diaz-Buxo JA**, Blumenthal S, Hayes D, Gores P, Gordon B. Galactosamine-induced fulminant hepatic necrosis in unanesthetized canines. *Hepatology* 1997; **25**: 950-957
- Miller DJ**, Hickman R, Fratter R, Terblanche J, Saunders SJ. An animal model of fulminant hepatic failure: a feasibility study. *Gastroenterology* 1976; **71**: 109-113
- Hanid MA**, Mackenzie RL, Jenner RE, Chase RA, Mellon PJ, Trewby PN, Janota I, Davis M, Silk DB, Williams R. Intracranial pressure in pigs with surgically induced acute liver failure. *Gastroenterology* 1979; **76**: 123-131
- Sussman NL**, Chong MG, Koussayer T, He DE, Shang TA, Whisennand HH, Kelly JH. Reversal of fulminant hepatic failure using an extracorporeal liver assist device. *Hepatology* 1992; **16**: 60-65
- Gardner CR**, Heck DE, Yang CS, Thomas PE, Zhang XJ, DeGeorge GL, Laskin JD, Laskin DL. Role of nitric oxide in acetaminophen-induced hepatotoxicity in the rat. *Hepatology* 1998; **27**: 748-754
- Gunawan BK**, Liu ZX, Han D, Hanawa N, Gaarde WA, Kaplowitz N. c-Jun N-terminal kinase plays a major role in murine acetaminophen hepatotoxicity. *Gastroenterology* 2006; **131**: 165-178
- Nakagawa H**, Maeda S, Hikiba Y, Ohmae T, Shibata W, Yanai A, Sakamoto K, Ogura K, Noguchi T, Karin M, Ichijo H, Omata M. Deletion of apoptosis signal-regulating kinase 1 attenuates acetaminophen-induced liver injury by inhibiting c-Jun N-terminal kinase activation. *Gastroenterology* 2008; **135**: 1311-1321
- Namisaki T**, Yoshiji H, Kojima H, Yoshiji J, Ikenaka Y, Noguchi R, Sakurai S, Yanase K, Kitade M, Yamazaki M, Asada K, Uemura M, Nakamura M, Fukui H. Salvage effect of the vascular endothelial growth factor on chemically induced acute severe liver injury in rats. *J Hepatol* 2006; **44**: 568-575
- Ma KF**, Yang HY, Chen Z, Qi LY, Zhu DY, Lou YJ. Enhanced expressions and activations of leukotriene C4 synthesis enzymes in D-galactosamine/lipopolysaccharide-induced rat fulminant hepatic failure model. *World J Gastroenterol* 2008; **14**: 2748-2756
- Brattin WJ**, Glende EA, Recknagel RO. Pathological mechanisms in carbon tetrachloride hepatotoxicity. *J Free Radic Biol Med* 1985; **1**: 27-38
- Chieli E**, Malvaldi G. Role of the microsomal FAD-containing monooxygenase in the liver toxicity of thioacetamide S-oxide. *Toxicology* 1984; **31**: 41-52
- Pallottini V**, Martini C, Bassi AM, Romano P, Nanni G, Trentalancia A. Rat HMGCoA reductase activation in thioacetamide-induced liver injury is related to an increased reactive oxygen species content. *J Hepatol* 2006; **44**: 368-374

- 35 **Matkowskyj KA**, Marrero JA, Carroll RE, Danilkovich AV, Green RM, Benya RV. Azoxymethane-induced fulminant hepatic failure in C57BL/6J mice: characterization of a new animal model. *Am J Physiol* 1999; **277**: G455-G462
- 36 **Bélanger M**, Côté J, Butterworth RF. Neurobiological characterization of an azoxymethane mouse model of acute liver failure. *Neurochem Int* 2006; **48**: 434-440
- 37 **Toritsu T**, Nakaya M, Watanabe S, Hashimoto M, Yoshida H, Chinen T, Yoshida R, Okamoto F, Hanada T, Torisu K, Takaesu G, Kobayashi T, Yasukawa H, Yoshimura A. Suppressor of cytokine signaling 1 protects mice against concanavalin A-induced hepatitis by inhibiting apoptosis. *Hepatology* 2008; **47**: 1644-1654
- 38 **Takada Y**, Ishiguro S, Fukunaga K, Gu M, Taniguchi H, Seino KI, Yuzawa K, Otsuka M, Todoroki T, Fukao K. Increased intracranial pressure in a porcine model of fulminant hepatic failure using amatoxin and endotoxin. *J Hepatol* 2001; **34**: 825-831
- 39 **Takada Y**, Ishiguro S, Fukunaga K. Large-animal models of fulminant hepatic failure. *J Artif Organs* 2003; **6**: 9-13
- 40 **Rahman TM**, Hodgson HJ. Animal models of acute hepatic failure. *Int J Exp Pathol* 2000; **81**: 145-157
- 41 **Zeneroli ML**, Cioni G, Crisi G, Vezzelli C, Ventura E. Globus pallidus alterations and brain atrophy in liver cirrhosis patients with encephalopathy: an MR imaging study. *Magn Reson Imaging* 1991; **9**: 295-302

S- Editor Sun H L- Editor Cant MR E- Editor Zhang DN